Kinetic Study of Retro-Aldol Condensation of Glucose to Glycolaldehyde with Ammonium Metatungstate as the Catalyst

Junying Zhang, Baolin Hou, Aiqin Wang, ZhenLei Li, Hua Wang, and Tao Zhang
State Key Laboratory of Catalysis, Dalian Institute of Chemical Physics, Chinese Academy of Sciences, Dalian 116023, China

DOI 10.1002/aic.14554
Published online July 15, 2014 in Wiley Online Library (wileyonlinelibrary.com)

The kinetics of the retro-aldol condensation of glucose to glycolaldehyde was studied in a batch reactor at 423–453 K using ammonium metatungstate (AMT) as the catalyst. Three consecutive reactions were considered: retro-aldol condensation of glucose to erythrose and glycolaldehyde (R1), retro-aldol condensation of erythrose to two moles of glycolaldehyde (R2), and further conversion of glycolaldehyde to side products (R3). Fitting of the experimental data showed that R1 was first-order reaction while R2 and R3 were 1.7th- and 2.5th-order reaction, respectively. Conversely, the reaction rate of R1 was 0.257th-order dependence on the concentration of AMT catalyst. The apparent activation energies for R1, R2, and R3 were 141.3, 79.9, and 52.7 kJ/mol, respectively. The high activation energy of R1 suggests that a high temperature is favorable to the formation of glycolaldehyde. The experimental C–t curves at different temperatures and initial glucose concentrations were well predicted by the kinetic model. © 2014 American Institute of Chemical Engineers *AIChE J*, 60: 3804–3813, 2014
Keywords: glucose, glycolaldehyde, retro-aldol condensation, kinetics, ethylene glycol

Introduction

With the diminishing petroleum reserves and the ever-increasing CO_2 emissions, exploration, and utilization of renewable resources has become a hot topic all over the world.[1–8] Biomass, as the only renewable carbon source on the earth, is being considered as a promising feedstock for the sustainable production of fuels and chemicals.[9–23] Cellulose is the most abundant biomass and accounts for 35–50 wt % of lignocellulosic materials.[12] Unlike starch, the inedible nature of cellulose allows for the extensive utilization without threatening the food supply. Therefore, the catalytic conversion of cellulose into fuels and chemicals is attracting increasing attentions from both academia and industry.

Cellulose is a polymer of glucose linked with β-1,4-glycosidic bonds. The extensive intra- and intermolecular hydrogen bonds make its structure rather stable against attack by foreign molecules. To facilitate the degradation of cellulose, pretty harsh reaction conditions or reagents (e.g., supercritical water, ball milling, concentrated sulfuric acid, and so forth) are often used,[24–29] which are associated with high investment on equipment or production of acidic waste water. With the assistance of solid catalysts and by coupling hydrolysis of cellulose with the subsequent hydrogenation/hydrogenolysis, conversion of cellulose into polyols can be accomplished in one pot under mild and environmentally benign conditions.[30–50] This process offers prominent advantages of high atom-economy since most of hydroxyl groups in the cellulose can be preserved in the target polyols.

Among various polyols, ethylene glycol (EG) shares the largest market (~20 million tonnes per year) as it can be used as monomers for production of polyethylene teraphthalate, one of the most important polymers in plastic industry.[51] In 2008, we for the first time reported the one-pot production of EG from cellulose using Ni-promoted tungsten carbide (W_2C) catalyst, and the EG yield was over 60 wt %.[32] The advantages of low-cost and renewable feedstock, high conversion, and selectivity to the end product EG, and operational simplicity inherited from one-pot reaction make this process attractive not only in fundamental science but also economically viable in industrial application,[39–41] thus may open a new avenue for the production of bio-EG. Nevertheless, this is a new reaction and many important issues need yet to be addressed. In the past 5 years, we have made progress in the catalyst optimization and reaction mechanism understanding. For example, using a three-dimensional mesoporous carbon as the support of tungsten carbide or using a postimpregnation procedure for preparation of Ni—W_2C catalyst, the EG yield could be enhanced further, exceeding 70%.[35,44] Moreover, we found that tungsten carbide was not mandatory for this reaction; instead, using bimetal catalysts composed of W and a transition metal (Ni, Ru, Pt, Pd, and so forth), a high yield of EG could also be achieved.[38] Further investigations on various tungsten compounds revealed that, whatever the starting tungsten compounds (W, WO_x, WC_x, H_2WO_4, heteropoly acids, and so forth), soluble tungsten bronze (H_xWO_3) was always formed during the reaction as a consequence of high-temperature water and pressurized H_2.[46] This soluble H_xWO_3

Correspondence concerning this article should be addressed to T. Zhang at taozhang@dicp.ac.cn or A. Wang at aqwang@dicp.ac.cn.

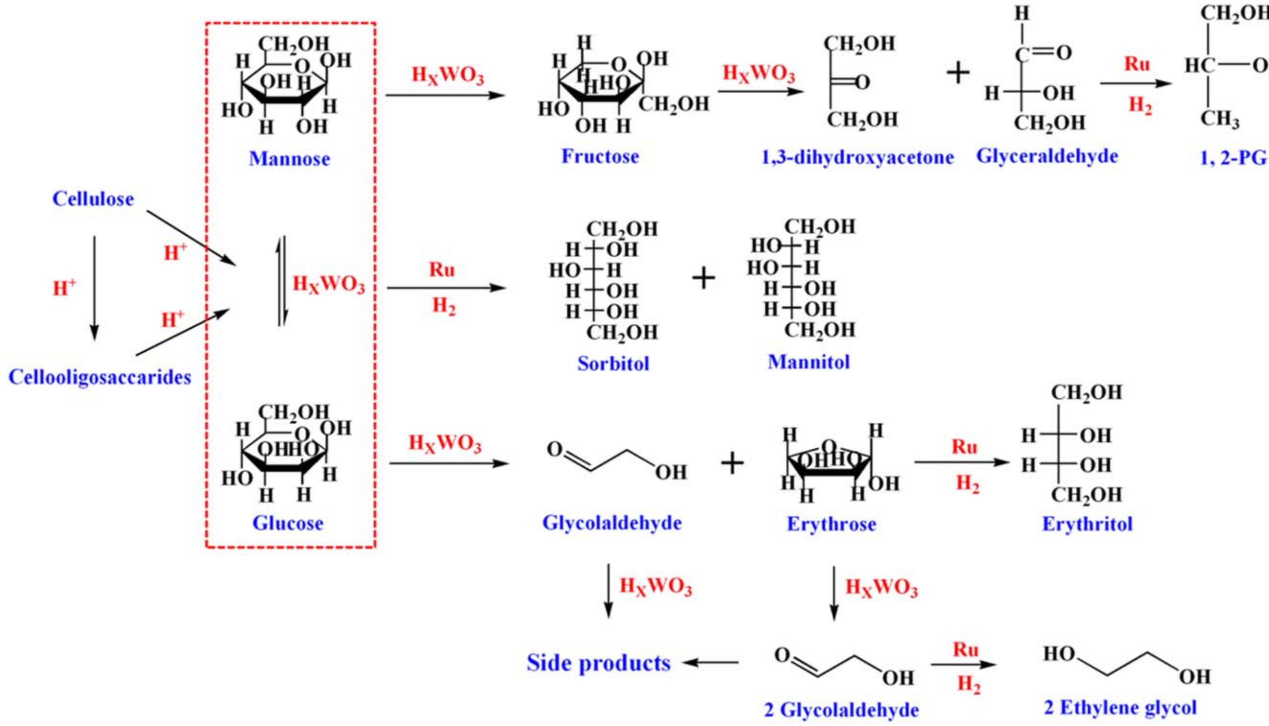

Figure 1. The reaction network of cellulose transformation with dual catalyst $H_xWO_3 + Ru$.

[Color figure can be viewed in the online issue, which is available at wileyonlinelibrary.com.]

is probably the catalytically active species for the selective cleavage of C—C bonds of cellulose-derived sugars.[51] Reactions with differently structured sugars (glucose and fructose) showed that the C—C cleavage followed well with the retro-aldol condensation pathway, producing glycolaldehyde as the intermediates.[39–41,51] When various tungsten species was used together with a transition metal (in particular Ni or Ru) to form a dual catalyst, the formed glycolaldehyde was instantly hydrogenated over transition metal to produce EG.[46,49,51] Therefore, the one-pot production of EG from cellulose is a cascade reaction composed of three reactions: (1) hydrolysis of cellulose to soluble celloligosaccharides and glucose with the catalysis of protons, which can be in situ generated by hot water or arise from tungsten acid, (2) C—C bond cleavage of cellulose-derived sugars via the retro-aldol reaction pathway with the catalysis of soluble tungsten species to produce glycolaldehyde, and (3) immediate hydrogenation of glycolaldehyde to form EG over the transition metal catalyst.[51] Figure 1 illustrates the whole reaction network involved in the cellulose transformation with dual catalyst $H_xWO_3 + Ru$, which clearly shows the complicated nature of the transformations. Besides the three main reactions, there are also a variety of side reactions arising from metastable sugars and glycolaldehyde that compete with the main reactions leading to the decrease in the selectivity to EG. For example, the isomerization of glucose to fructose and the hydrogenation of glucose to hexitols (sorbitol and mannitol) can occur competitively with glucose retro-aldol condensation, and the fructose can further undergo retro-aldol condensation to form 1,3-dihydroxyacetone and glyceraldehyde, the latter two are hydrogenated to 1,2-Propanediol (PG). Conversely, the aldehydes (glycolaldehyde, glyceraldehyde, and so forth) are not stable in hot water; if not being instantly hydrogenated to more stable polyols, they are subject to other transformations such as condensation to higher molecular aldehydes byproducts. Based on our previous work,[46,51] under optimized reaction conditions (518 K, 6 MPa H_2, 1 wt % cellulose, H_xWO_3/cellulose = 1/10 (w/w), Ni/W = 1 or Ru/W = 0.1) microcrystalline cellulose could be completely converted in 0.5 h and the yield of the target product EG was 50–70%; other byproducts contained C3 polyols (1,2-PG and glycerol, in total ~10%), C4 polyols (1,2-butanediol and erythritol, in total 5–10%), C6 polyols (sorbitol and mannitol, 5–10%), unidentified compounds (5–25%) and gas phase (CO_2, methane, and so forth, ~2%). The formation of a variety of byproducts presents a great challenge for separation, especially when the polyols have very near boiling points or form azeotrope with water. Therefore, the enhancement in the selectivity to the target product, for instance, through optimization of the catalyst formulations and operational parameters, is very important for this process. To provide an insightful understanding of the key factors controlling the selectivity as well as to provide the basis for reactor and process design, kinetic study must be conducted although it is unreasonably ignored in most of current biomass catalysis works. Due to many parallel and competitive reactions involved in this one-pot process as well as the difficulty in identifying the intermediates, the kinetic study of this reaction still presents a significant challenge.

Conversely, glucose is a basic unit of cellulose and other sugar polymers and can be easily obtained by hydrolysis of cellulose and hemicellulose. One can see from Figure 1 that glucose is an important intermediate in the process of cellulose conversion to EG and starting from glucose can greatly simplify the kinetic study of the whole network. Moreover, glucose itself can be considered as a potential promising feedstock for the production of EG due to its availability on a large scale and capability for continuous processing.[52,53] Therefore, the kinetic study of glucose transformation to EG

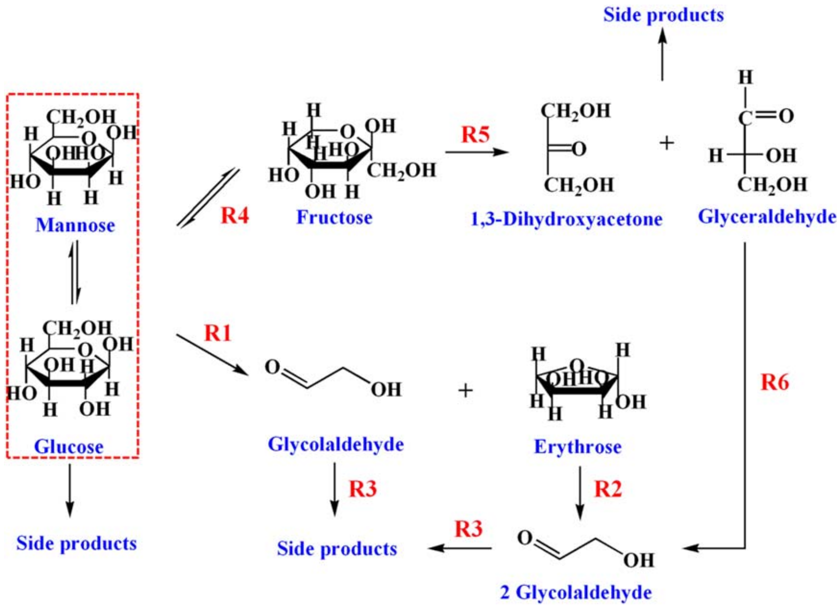

Scheme 1. The reaction network of glucose conversion with AMT as the catalyst.

[Color figure can be viewed in the online issue, which is available at wileyonlinelibrary.com.]

not only provides the fundamental understanding of cellulose conversion but also is of highly practical importance.

Herein, we report for the first time our detailed study on the kinetics of glucose conversion to EG. For clarity, the whole work is divided into two PARTS. In PART I, we describe the kinetics from glucose to glycolaldehyde with soluble W compound as the catalyst because this reaction is the key to understanding C—C cleavage of glucose. In PART II, we describe the kinetics from glycolaldehyde to EG through hydrogenation, and in particular focus on the influence of W species on the hydrogenation rate of glycolaldehyde over metallic Ru center.

Reaction Model

To simplify the kinetic study, we assume a dual catalyst center mechanism where the selective cleavage of C—C bonds in glucose occurs only with the soluble tungsten species via a retro-aldol reaction pathway,[51] and the presence of hydrogenation catalyst such as Ru does not affect the retro-aldol reaction rate. The control experiment with Ru/C as the single catalyst showed that the products from the C—C bond cleavage were less than 5% when the reaction temperature was lower than 473 K,[46] confirming that our assumption is reasonable. Accordingly, in this kinetic study, the water soluble ammonium metatungstate (AMT) was used as the sole catalyst.

Scheme 1 shows the reaction network of the catalytic conversion of glucose with AMT, which includes both parallel and successive reactions. Since mannose is derived from glucose via epimerization[54] and it also undergoes retro-aldol condensation reaction as glucose does, we simply consider it as glucose in the kinetic study. With this assumption, two competitive reactions take place in the primary reactions: retro-aldol condensation of glucose to form equal-molar erythrose and glycolaldehyde (R1), and isomerization of glucose to fructose (R4). However, the products from the primary reactions are not stable and subject to undergoing secondary reactions. In the secondary reactions, erythrose undergoes retro-aldol condensation to form two moles of glycolaldehyde (R2), which can be further converted to undesired products (R3). Similarly, fructose also undergoes retro-aldol condensation reactions (R5) to form 1,3-dihydroxyacetone and glyceraldehyde that further undergo retro-aldol condensation to form glycolaldehyde (R6) or transform to other byproducts. Such a complicated reaction network will make the kinetic study quite difficult. Therefore, simplification must be conducted. Based on the experimental data of cellulose conversion under the copresence of tungstic acid and Ru/C,[46] the total yields of 1,2-propylene glycol and glycerol were always lower than 10 wt %, which was only 1/5 of the EG yield. This result suggests that the contribution of the reactions R4–R6 to the formation of glycolaldehyde is very minor in comparison with the glucose retro-aldol condensation route (R1 and R2) so that their influence on the kinetics of the key intermediate glycolaldehyde can be ignored. Thus, the kinetic model for the glucose conversion with AMT is greatly simplified, as illustrated in Scheme 2 where only three reactions (R1, R2, and R3) are involved.

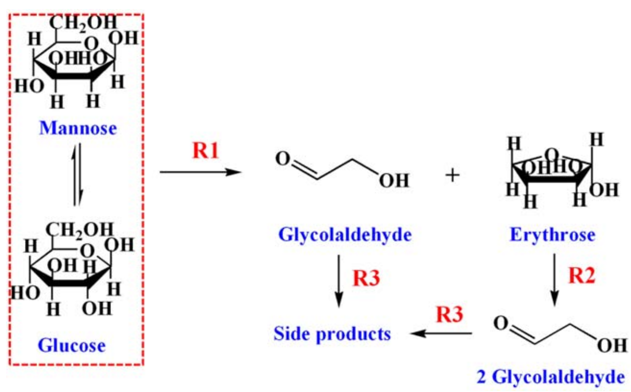

Scheme 2. The simplified kinetic model for glucose conversion to glycolaldehyde with AMT as the catalyst.

[Color figure can be viewed in the online issue, which is available at wileyonlinelibrary.com.]

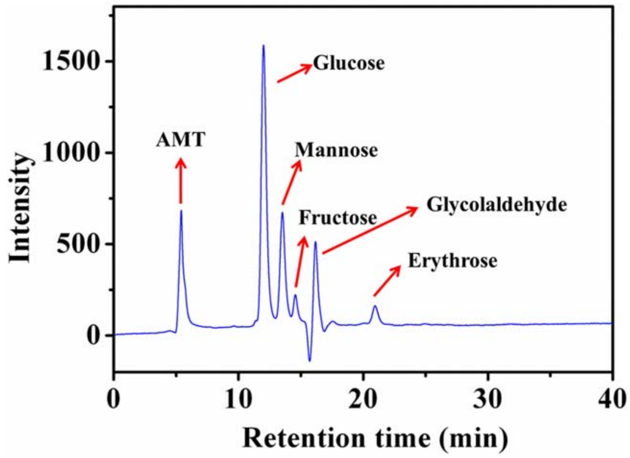

Figure 2. A typical HPLC graph for the glucose conversion with the catalysis of AMT.

The negative peak is caused by the sampling valve contamination, and the possible error in the peak quantification is minimized by using external standard method. [Color figure can be viewed in the online issue, which is available at wileyonlinelibrary.com.]

Based on our previous studies,[46,51] the retro-aldol condensation of glucose with soluble tungsten species is homogeneous reaction. Furthermore, we assume that the above three reactions are all irreversible and the concentration of AMT keeps constant throughout the reaction. With these assumptions, the following differential equations can be derived

$$\frac{dC_{\mathrm{G}}}{dt} = -k_1 C_{\mathrm{G}} \tag{1}$$

$$\frac{dC_{\mathrm{E}}}{dt} = k_1 C_{\mathrm{G}} - k_2 C_{\mathrm{E}}{}^{n_{\mathrm{E}}} \tag{2}$$

$$\frac{dC_{\mathrm{GA}}}{dt} = k_1 C_{\mathrm{G}} + 2k_2 C_{\mathrm{E}}{}^{n_{\mathrm{E}}} - k_3 C_{\mathrm{GA}}^{n_{\mathrm{GA}}} \tag{3}$$

where C_{G}, C_{E}, and C_{GA} are the concentrations (mol/m^3) of glucose, erythrose, and glycolaldehyde, respectively, k_i ($i = 1, 2, 3$) are the rate constants of the three reactions, and n_{E}, n_{GA} are the reaction orders of R2 and R3 with respect to erythrose and glycolaldehyde, respectively.

The rate constant, k_i, is dependent on temperature and AMT concentration according to Arrhenius equation

$$k_i = k_0\ C_{\mathrm{AMT}}^{n_{\mathrm{AMT}}} = A\mathrm{e}^{-\frac{E_a}{RT}} \tag{4}$$

$$A = A_0 C_{\mathrm{AMT}}^{n_{\mathrm{AMT}}} \tag{5}$$

where A is the pre-exponential factor; E_a is the activation energy (kJ/mol); R is the ideal gas law constant (8.3143 $\times$ 10^{-3} kJ/mol K); T is the temperature (K); C_{AMT} is the concentration of AMT (mol/m^3); n_{AMT} is the reaction order with respect to AMT concentration.

Experiments

In all experiments, glucose (J & K Chemical), AMT (Sinopharm Chemical Reagent Co.), and glycolaldehyde (Chemfun Medical Technology Co., Shanghai) were used as received. Based on our previous study,[52] the glucose or glycolaldehyde transformation reactions were performed in a stainless-steel autoclave (Parr Instrument Company, 300 mL) which is equipped with sampling tube, stirring impeller, and temperature and pressure control system. Typically, 0.05 g AMT was dissolved in 140 mL water and the resulting solution was put into the autoclave. The autoclave was flushed with H_2 five times and then pure H_2 gas was charged until the pressure of 6 MPa. The autoclave was then heated to the desired temperature, into which 10 mL of an aqueous solution of glucose or glycolaldehyde was fed by a Shimadzu LC pump (LC-20A) at a flow rate of 10 mL/min. It took 1 min to finish the feeding process, and this point was considered as the initial time ($t = 0$). Then, the reaction was started by strong agitation at 1100 rpm. Samples were taken from the reactor at a certain time interval for analysis.

After filtration through a 0.45 μm Polytetrafluoroethylene filter, the liquid samples were analyzed with a high performance liquid chromatograph (HPLC, Aglient 1200) in combination with HPLC-Mass spectroscopy, with water as the mobile phase and RI as the detector. For the separation of polyols, a Shodex SC100 column was used with water flow rate of 0.6 mL/min and column temperature of 348 K. For the separation of unsaturated intermediates, a CARBO-Sep CHO-620 column was used with water flow rate of 0.4 mL/min and column temperature of 353 K. The

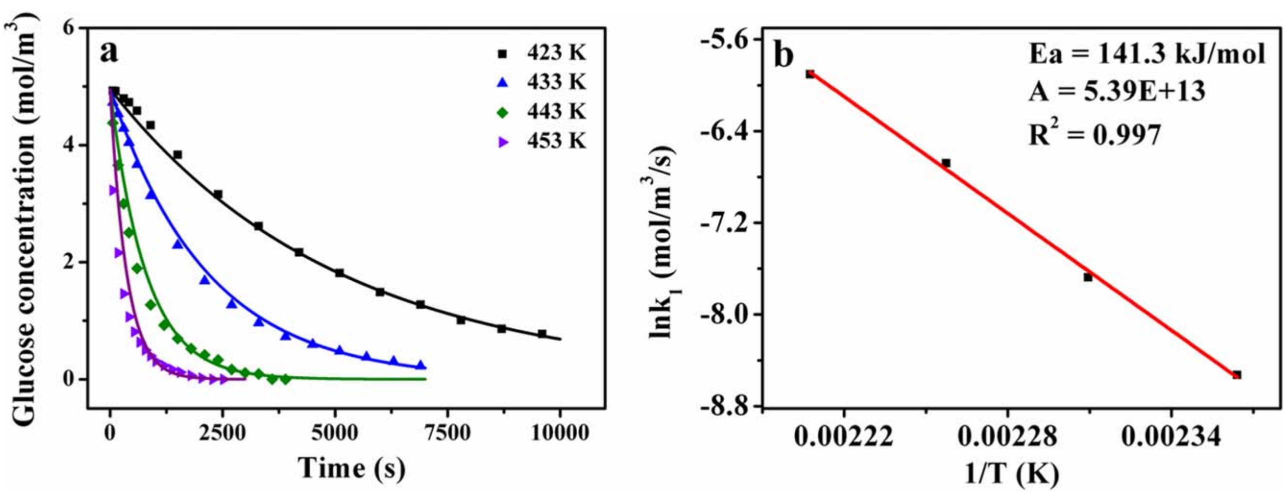

Figure 3. Kinetics of retro-aldol condensation of glucose under AMT catalyst.

(a) Glucose concentration vs. reaction time at different temperatures; (b) Arrhenius plot showing the temperature dependence of rate constant (k_1) for estimation of activation energy (E_{a1}). Symbols are experimental data and lines are fitted curves. [Color figure can be viewed in the online issue, which is available at wileyonlinelibrary.com.]

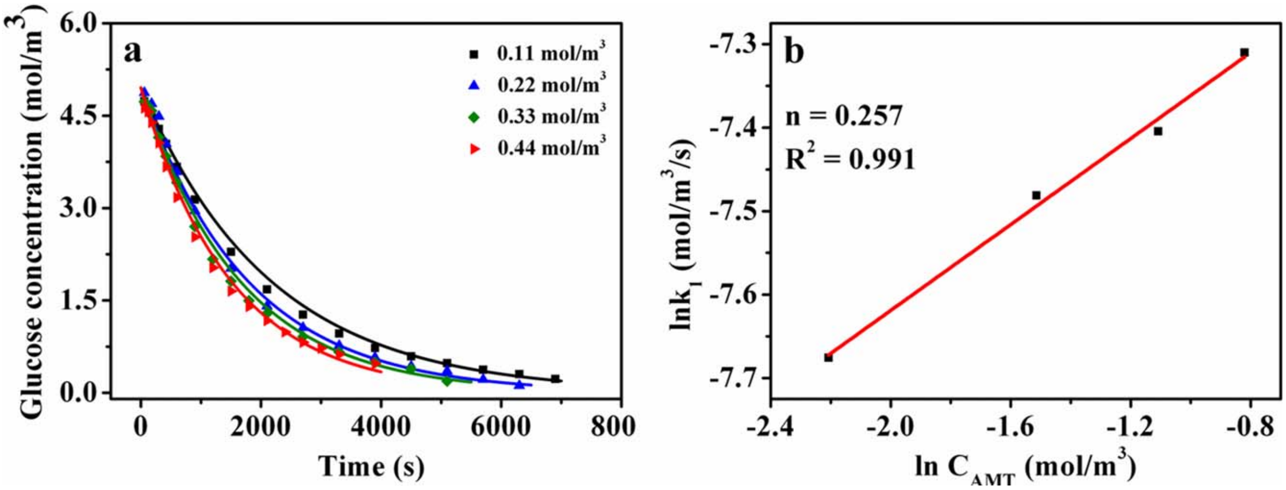

Figure 4. Dependence of the reaction rate on the catalyst amount.

(a) Glucose concentration vs. reaction time at different AMT concentrations; (b) lnk_1–ln C_{AMT} plot. T = 433 K, C_{G0} = 4.96 mol/m^3. [Color figure can be viewed in the online issue, which is available at wileyonlinelibrary.com.]

quantification of intermediates and products was made by an external standard method.

Results and Discussion

Kinetics of glucose retro-aldol condensation (R1)

The kinetic study of retro-aldol condensation of glucose (R1) was conducted in the temperature range of 423–453 K with the presence of a constant concentration of catalyst AMT (0.11 mol/m^3) and H_2. Although H_2 is supposed to have no effect on the retro-aldol reaction of glucose without the presence of a hydrogenation component, it may affect the chemistry of catalyst AMT.[51] Therefore, H_2 was always added in the kinetic studies. Figure 2 shows the typical HPLC graph of glucose transformation under the catalysis of AMT, from which one can clearly see that there are fructose, mannose, erythrose, glycolaldehyde, and unidentified byproduct in addition to AMT catalyst and unreacted glucose, and the carbon balance between the liquid products and the initial glucose input is better than 96%. The glucose concentrations with the reaction time at different temperatures were fitted with first-order equation

$$C_G = C_{G0}e^{-k_1 t} \tag{6}$$

The rate constant (k_1) in the equation was determined by nonlinear least-squares fitting of the experimental data using

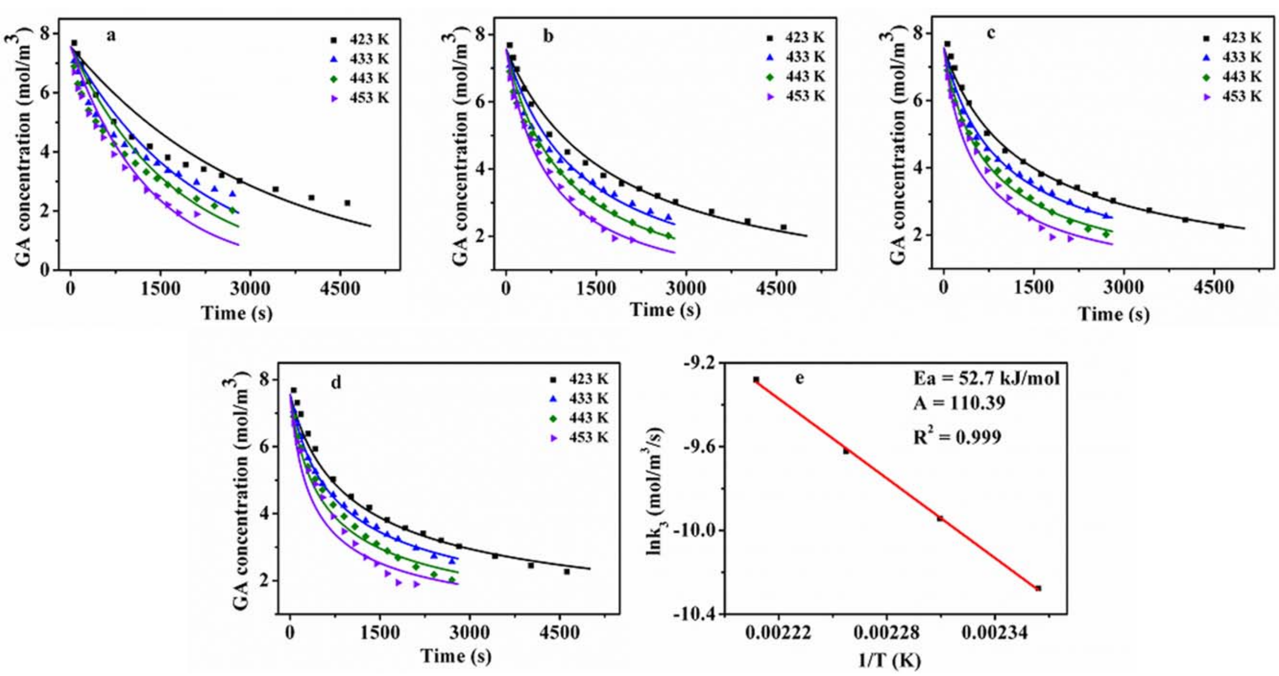

Figure 5. Glycolaldehyde concentration with reaction time (symbols) as well as the fitting result (lines) with different reaction models.

(a) First-order; (b) second-order; (c) 2.5th-order; (d) third-order; (e) Arrhenius plot based on 2.5th model. Reaction conditions: C_{GA0} = 7.56 mol/m^3 and C_{AMT} = 0.11 mol/m^3. [Color figure can be viewed in the online issue, which is available at wileyonlinelibrary.com.]

Table 1. The Standard Deviation Between Experimental Data and Fitting Result by Different Reaction Order for Glycolaldehyde Degradation.

	$\mathbf{R} = \sum_{i=0}^{n}\left(\left(C_{i,\text{model}}-C_{i,\exp}\right)/C_{i,\exp}\right)^2$			
Reaction order	423 K	433 K	443 K	453 K
1	0.2860	0.2456	0.2780	0.1494
2	0.0290	0.0376	0.0199	0.0240
2.5	0.0095	0.0080	0.0181	0.0752
3	0.0288	0.0078	0.0597	0.1620

Microsoft Excel Solver pack as described by Kemmer and Keller.[55] As shown in Figure 3a, all the experimental data obtained at $C_{G0} = 4.96$ mol/m^3 and $C_{AMT} = 0.11$ mol/m^3 were well-fitted with first-order kinetic equation, proving that the retro-aldol condensation reaction of glucose follows the first-order kinetics. Arrhenius parameters including apparent activation energy (E_a) and pre-exponential coefficients (A) were determined by plotting natural log of rate constants (k_1) vs. reciprocal of temperature (K), as shown in Figure 3b. The high apparent activation energy (141.3 kJ/mol) suggests that the retro-aldol reaction of glucose is highly sensitive to the reaction temperature and a high reaction temperature will be favorable to the C—C bond cleavage of glucose. Meanwhile, a high pre-exponential coefficient (5.39 E +13) is in good agreement with homogeneous catalysis.

Since the reaction rate constant (k_1) is not only a function of reaction temperature (T), but also a function of catalyst concentration in the case of homogeneous catalysis,[56] we subsequently investigated the effect of catalyst concentration. The dependence of the reaction rate on the concentration of AMT is illustrated in Figure 4a. The experimental data were obtained at $T = 433$ K, $C_{G0} = 4.96$ mol/m^3, and $C_{AMT} = 0.11$, 0.22, 0.33, and 0.44 mol/m^3. According to the equation $k = k_0 C_{AMT}^{n_{AMT}}$, n_{AMT} is obtained from the slope of plot ln k_1 –ln C_{AMT} shown in Figure 4b. $n_{AMT} = 0.257$ indicates that the reaction rate increases nonlinearly with the catalyst amount. Assuming that the C—C cleavage of glucose proceeds via the complexing of OH groups with W,[57,58] the 0.257 dependence may imply that one AMT molecule can complex approximately four glucose molecules. This information is very important to the study of glucose hydrogenation in the presence of AMT, as addressed in the PART II.

Kinetics of glycolaldehyde (GA) conversion to side products

Under hydrothermal conditions, glycolaldehyde is not stable and subject to various undesired reactions such as condensation and oxidation.[59–61] To obtain the kinetics of the undesired reaction of glycolaldehyde and its effect on the overall kinetics from glucose to EG, we conducted the kinetic experiments of glycolaldehyde conversion. The reaction temperature range investigated was the same as that for glucose conversion (423–453 K), and the initial concentrations of glycolaldehyde and AMT were 7.56 and 0.11 mol/m^3, respectively. The experimental data were fitted with different reaction models using Microsoft Excel Solver pack,[55] and deviation of the fitting result from experimental data were evaluated by sensitivity analysis. As shown in Figure 5 and Table 1, the first-order reaction model cannot well-describe the glycolaldehyde conversion; especially at lower temperatures the standard deviation value reaches 0.2860. Comparing the effect of reaction orders with respect to glycolaldehyde concentration one can see that the second or 2.5th-order reaction model can well-describe the reaction kinetics, and the 2.5th-order reaction model appears the best.

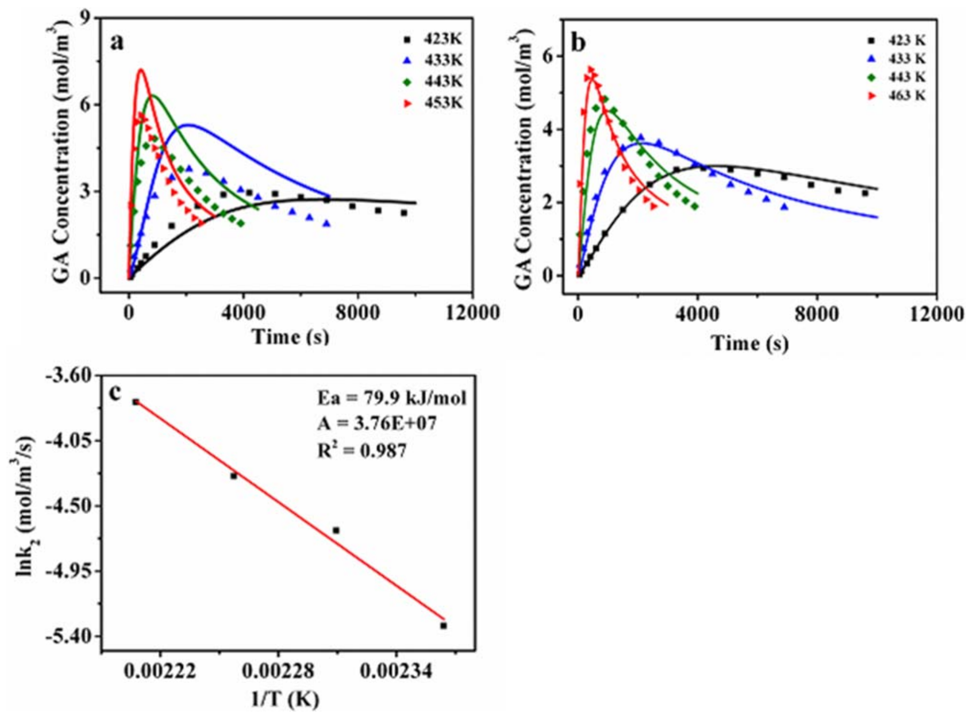

Figure 6. The experimental (symbols) and fitting (lines) results of glycolaldehyde concentration during glucose conversion by using different kinetic model of erythrose retro-aldol condensation.

(a) First-order; (b) 1.7th-order; and (c) Arrhenius plot of erythrose retro-aldol condensation based on 1.7th-order model. [Color figure can be viewed in the online issue, which is available at wileyonlinelibrary.com.]

Table 2. Rate Constants for the Three Consecutive Reactions and Arrhenius Parameters

Reaction	Rate constants k_i			Reaction order (n)	E_a (kJ/mol)	A
	423 K	463 K	503 K			
R1	1.94 E−04	6.24 E−03	1.16 E−01	1.0	141.3	5.39 E+13
R2	5.08 E−03	3.62 E−02	1.89 E−01	1.7	79.9	3.76 E+07
R3	3.42 E−05	1.25 E−04	3.71 E−04	2.5	52.7	110.39

This result indicates that the undesired reaction of glycolaldehyde involves two- or more molecules, most probably the condensation reaction.[59–61] Based on the 2.5th-order reaction model, the apparent activation energy and pre-exponential coefficient were estimated to be 52.7 kJ/mol and 110.39, respectively. The low apparent activation energy and the high reaction order dependence suggests that the glycolaldehyde is easy to undergo further undesirable transformations even at low temperatures and the undesired reaction rate will be greatly accelerated at high concentrations of glycolaldehyde. Therefore, to avoid the side reactions associated with glycolaldehyde, the glycolaldehyde concentration must be kept at a low value, which can be accomplished using semi-continuous reactor[52] or by coupling with the rapid subsequent reactions such as hydrogenation to EG.[51]

Kinetics of erythrose retro-aldol condensation

Since the chemically pure erythrose is not available, the kinetics of erythrose conversion cannot be obtained directly using erythrose as the feedstock. Nevertheless, based on the fact that the glucose retro-aldol condensation follows the first-order kinetics and the erythrose is similar to glucose in molecular structure, we first assume that the erythrose retro-aldol condensation also follows the first-order kinetics. Thus, by solving the Eqs. 1 and 2, the integrated rate equations for the concentration of glucose and erythrose are obtained

$$C_G = C_{G0}e^{-k_1 t} \tag{7}$$

$$C_E = \frac{k_1 C_{G0}}{k_2 - k_1}\left(e^{-k_1 t} - e^{-k_2 t}\right) \tag{8}$$

and the differential equation for glycolaldehyde can be described as

$$\frac{dC_{GA}}{dt} = k_1 C_{G0}e^{-k_1 t} + \frac{2k_2 k_1 C_{G0}}{k_2 - k_1}\left(e^{-k_1 t} - e^{-k_2 t}\right) - k_3 C_{GA}^{n_{GA}} \tag{9}$$

This kinetic model was used to fit the experimental data obtained at 423–453 K for glucose conversion under the

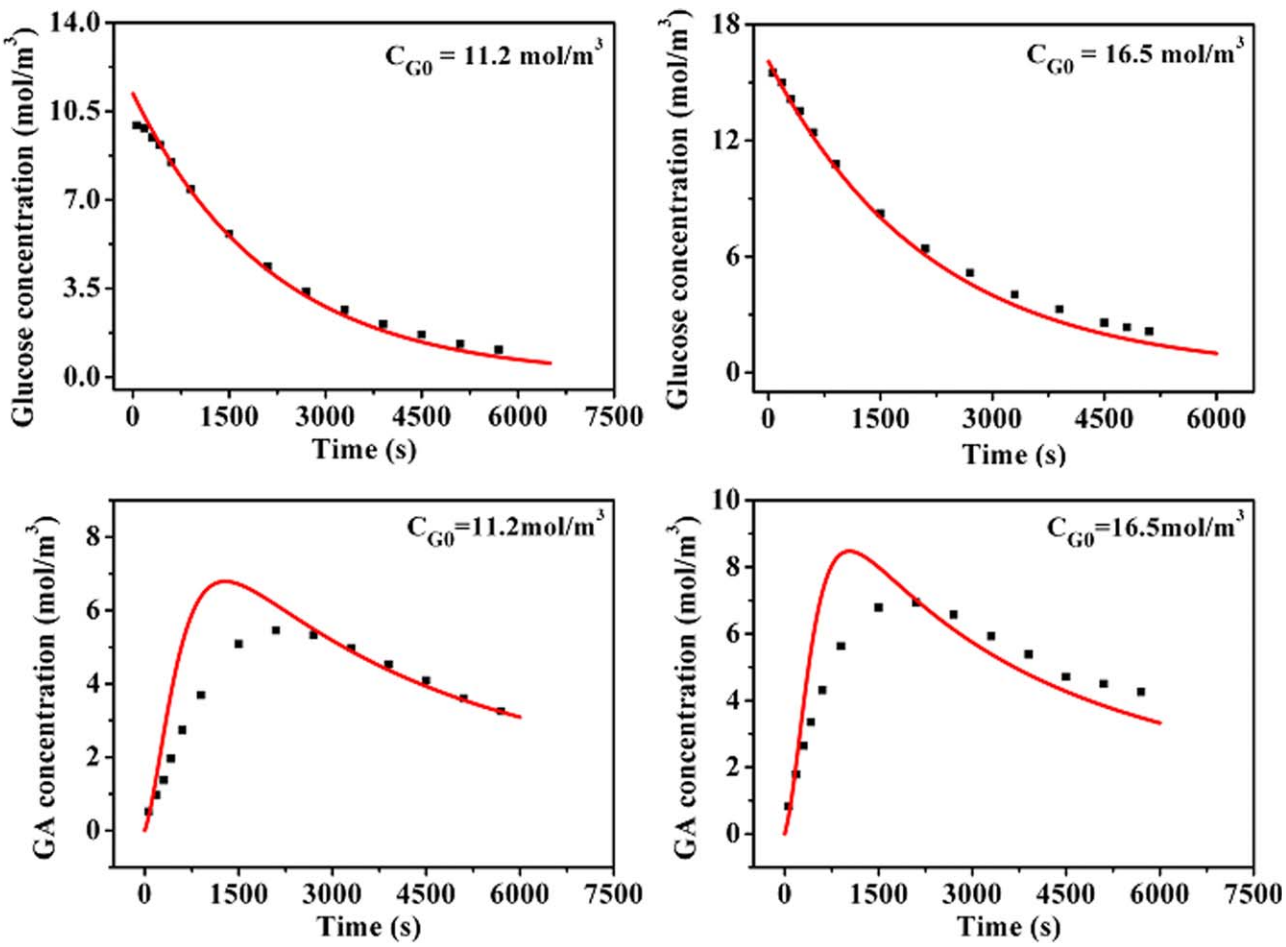

Figure 7. Experimental (dots) and calculated (lines) results for the overall reaction of glucose at different initial concentration of glucose.

T = 433 K. [Color figure can be viewed in the online issue, which is available at wileyonlinelibrary.com.]

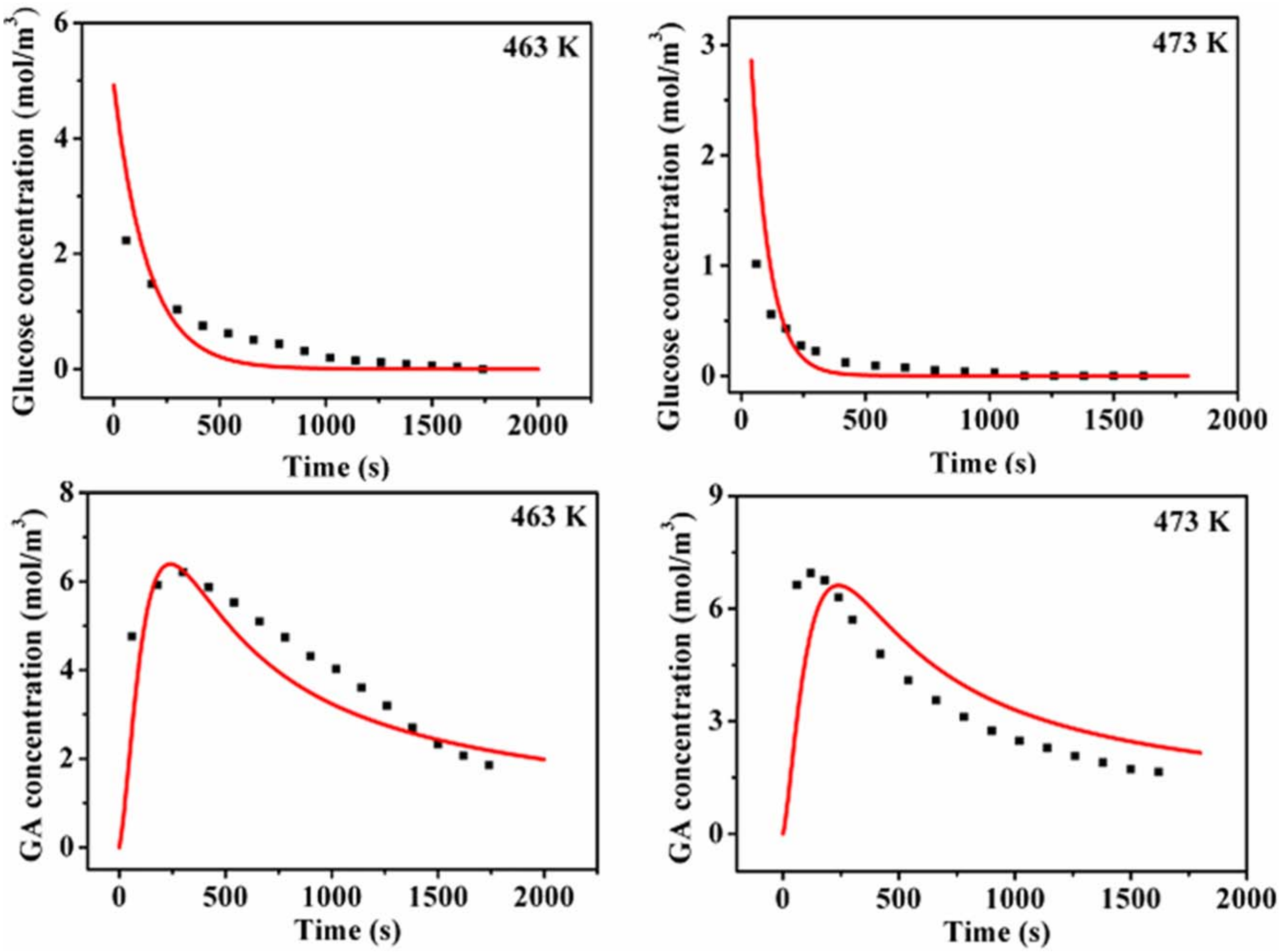

Figure 8. Experimental (dots) and calculated (lines) results for the overall reaction of glucose at different temperatures.
$C_{G0} = 4.96$ mol/m^3. [Color figure can be viewed in the online issue, which is available at wileyonlinelibrary.com.]

catalysis of AMT. Figure 6a shows the fitting result of glycolaldehyde concentration with the reaction time. It can be seen that this first-order reaction model does not match the experiment. Therefore, the reaction model must be modified, and a new kinetic model assuming the reaction order of n_E is proposed

$$\frac{dC_{GA}}{dt} = k_1C_{G0}e^{-k_1t}+2k_2\left[\frac{k_1C_{G0}}{k_2-k_1}\left(e^{-k_1t}-e^{-k_2t}\right)\right]^{n_E}-k_3C_{GA}{}^{n_{GA}} \tag{10}$$

Figure 6b shows the fitting result based on the new kinetic model wherein the reaction order (n_E) is determined to be 1.7th, and it matches the experimental data very well. It should be mentioned that this partial reaction order is obtained by fitting the experimental data of glucose transformation to glycolaldehyde, hence any discrepancy from the simplified model shown in Scheme 2 will bring about the changes in the apparent activation energy and reaction order of R2. For example, erythrose may undergo other reactions in addition to retro-aldol condensation, such as condensation with other aldehydes, which is not considered in the simplified model. Conversely, the kinetic parameters for R1 and R3 also affect greatly the apparent reaction order of R2 according to Eq. 10. Therefore, the partial reaction order of R2 does not mean that the retro-aldol condensation of erythrose follows truly the 1.7th reaction order; instead, it is only an apparent reaction order. The Arrhenius parameters for erythrose retro-aldol condensation reaction were estimated based on the plot in Figure 6c. It can be seen that the apparent activation energy of retro-aldol condensation for erythrose ($E_a = 79.9$ kJ/mol) is much lower than that for glucose (141.3 kJ/mol), suggesting that the former molecule has the higher reactivity. Experimentally, the erythrose concentration was very low especially at a higher temperature or a longer time when glucose was used as the feedstock, which is in good agreement with the lower apparent activation energy of erythrose transformation.

Model validation

The kinetic models for the three consecutive reactions (glucose retro-aldol condensation reaction, erythrose retro-aldol condensation reaction, and glycolaldehyde conversion to side products) were verified by the overall reaction of glucose transformation to glycolaldehyde under the presence of AMT catalyst. Table 2 summarizes the rate constants at different temperatures and Arrhenius parameters, which were used for validation of the kinetic models. Figure 7 shows the experimental data obtained at different initial concentrations of glucose (11.2 and 16.5 mol/m^3) as well as the calculation results based on the kinetic parameters. For the glucose concentration with time course, good agreement was found between predicted and experimental results. However, for the glycolaldehyde concentration with the reaction time, it can be seen that the predicted maximum glycolaldehyde concentration is higher than the experimental values. One possible reason for this disagreement is the simplification in the kinetic model establishment. From

Figure 2, one can see that the isomerization of glucose to fructose always occur under the reaction conditions although to a less significant extent, and the subsequent retro-aldol reaction of fructose takes place too. In our model simplification, the two reactions were not considered, which would lead to overestimation of the glycolaldehyde production. Conversely, in our experiment not all the condensation products were quantified, as evidence by the fact that the carbon balance was always lower than 100%. This may also cause the experimental data error, and in turn the disagreement between predicted and experimental values. Nevertheless, our simplified model could well predict the overall trend of the target product glycolaldehyde, which is indeed encouraging given that the overall reaction from glucose to glycolaldehyde is rather complicated.

Figure 8 shows the experimental and predicted results at different temperatures (463 and 473 K). Similarly, better agreement was found for the glucose concentration than glycolaldehyde with the time course, but the overall trend was well predicted, validating the three kinetic models. One point to be noticed is that the predicted maximum value of glycolaldehyde concentration is lower than the experimental one. One possible reason for this discrepancy is that the reaction order of R3 is sensitive to the reaction temperature. As shown in Figure 5, when the reaction temperature is higher than 443 K, 2.5th-order kinetic model can no longer fit the experimental data well; instead, the second- or even the first-order kinetic model would fit better.

Conclusion

The retro-aldol condensation of glucose to glycolaldehyde under the catalysis of AMT is a key reaction in the direct conversion of cellulose to EG. This reaction is composed of two main reactions and several side reactions. In this kinetic study, simplifications were made by considering only three consecutive reactions: retro-aldol condensation of glucose to form erythrose and glycolaldehyde (R1), retro-aldol condensation of erythrose to form two moles of glycolaldehyde (R2), and glycolaldehyde further conversion to side products (R3). The experiments for kinetic study were conducted with a batch reactor. The results showed that the R1 is first-order dependence with respect to glucose concentration with an apparent activation energy of 141.3 kJ/mol, while the R2 and R3 are 1.7th- and 2.5th-order with an apparent activation energy of 79.9 and 52.7 kJ/mol, respectively. The experimental data at different initial concentration of glucose and at different temperatures were well-modelled with the above kinetic parameters, validating the kinetic models. This kinetic study indicates that high temperatures are favorable to the retro-aldol condensation of glucose to selectively form glycolaldehyde, while the concentration of glycolaldehyde in the reactor should always be kept at a very low value to avoid the condensation side reaction. This information is very important to the reactor design and optimization of operation conditions for the large-scale production of glycolaldehyde or EG from glucose or cellulose.

Acknowledgments

This work is supported by the National Natural Science Foundation of China (Grants 21176235 and 21206159).

Notation

C_{G0} = the initial glucose concentration, mol/m^3
C_G = concentration of glucose, mol/m^3
C_E = concentration of erythrose, mol/m^3
C_{GA} = concentration of glycolaldehyde, mol/m^3
C_{AMT} = concentration of AMT, mol/m
k_i = reaction rate constant that incorporate the AMT concentration for reactions R1–R3 (mol/m^3/s)
k_0 = reaction rate constant that does not include the AMT concentration (s^{-1})
E_a = apparent activation energy for reactions R1–R3
R = universal gas constant [8.314 J mol^{-1} K^{-1}]
T = temperature, K
n_E = reaction order with respect to erythrose concentration
n_{GA} = reaction order with respect to glycolaldehyde concentration
n_{AMT} = reaction order with respect to AMT concentration

Literature Cited

1. Huber GW, Iborra S, Corma A. Synthesis of transportation fuels from biomass: chemistry, catalysts, and engineering. *Chem Rev*. 2006;106:4044–4098.
2. Corma A, Iborra S, Velty A. Chemical routes for the transformation of biomass into chemicals. *Chem Rev*. 2007;107:2411−2502.
3. Rinaldi R, Schüth F. Design of solid catalysts for the conversion of biomass. *Energy Environ Sci*. 2009;2:610–626.
4. Marquardt W, Harwardt A, Hechinger M, Kraemer K, Viell J, Voll A. The biorenewables opportunity—toward next generation process and product systems. *AIChE J*. 2010;56(9):2228–2235.
5. Zhou C, Xia X, Lin C, Tong D, Beltramini J. Catalytic conversion of lignocellulosic biomass to fine chemicals and fuels. *Chem Soc Rev*. 2011;40:5588–5617.
6. Kobayashi H, Komanoya T, Guha SK, Hara K, Fukuoka A. Conversion of cellulose into renewable chemicals by supported metal catalysis. *Appl Catal A* 2011;409:13–20.
7. Gallezot P. Conversion of biomass to selected chemical products. *Chem Soc Rev*. 2012;41:1538–1558.
8. Wang Y, Deng W, Wang B, Zhang Q, Wan X, Tang Z, Wang Y, Zhu C, Cao Z, Wang G, Wan H. Chemical synthesis of lactic acid from cellulose catalysed by lead(II) ions in water. *Nat Commun*. 2013;4:1–7.
9. Dhepe PL, Fukuoka A. Cellulose conversion under heterogeneous catalysis. *ChemSusChem*. 2008;1:969–975.
10. Zhao C, Kou Y, Angeliki A, Lemonidou, Li X, Lercher JA. Highly selective catalytic conversion of phenolic bio-oil to alkanes. *Angew Chem Int Ed*. 2009;48:3987–3990.
11. Rangarajan S, Bhan A, Daoutidis P. Rule-based generation of thermochemical routes to biomass conversion. *Ind Eng Chem Res*. 2010; 49(21):10459–10470.
12. Alonso DM, Bond JQ, Dumesic JA. Catalytic conversion of biomass to biofuels. *Green Chem*. 2010;12:1493–1513.
13. Zhao C, Camaioni DM, Lercher JA. Selective catalytic hydroalkylation and deoxygenation of substituted phenols to bicycloalkanes. *J Catal*. 2012;288:92–103.
14. Peng B, Yuan X, Zhao C, Lercher JA. Stabilizing catalytic pathways via redundancy: selective reduction of microalgae oil to alkanes. *J Am Chem Soc*. 2012;134:9400−9405.
15. Daoutidis P, Marvin WA, Rangarajan S, Torres AI. Engineering biomass conversion processes: a systems perspective. *AIChE J*. 2013; 59:3–18.
16. Li G, Li N, Li S, Wang A, Cong Y, Wang X, Zhang T. Synthesis of renewable diesel with hydroxyacetone and 2-methyl-furan. *Chem Commun*. 2013;49:5727–5729.
17. Yang J, Li N, Li G, Wang W, Wang A, Wang X, Cong Y, Zhang T. Solvent-free synthesis of C10 and C11 branched alkanes from furfural and methyl isobutyl ketone. *ChemSusChem*. 2013;6:1149–1152.
18. Wang Y, Jin F, Sasaki M, Wahyudiono, Wang F, Jing Z, Goto M. Selective conversion of glucose into lactic acid and acetic acid with copper oxide under hydrothermal conditions. *AIChE J*. 2013;59: 2096–2104.
19. Wang J, Ren J, Liu X, Lu G, Wang Y. High yield production and purification of 5-Hydroxymethylfurfural. *AIChE J*. 2013;59:2558–2566.
20. Joffres B, Lorentz C, Vidalie M, Laurenti D, Quoineaud AA, Charon N, Daudin A, Quignard A, Geantet C. Catalytic hydroconversion of a wheat straw soda lignin: characterization of the products and the lignin residue. *Appl Catal B* 2014;145:167–176.
21. Yoshikawa T, Shinohara S, Yagi T, Ryumon N, Nakasaka Y, Tago T, Masuda T. Production of phenols from lignin-derived slurry liquid using ironoxide catalyst. *Appl Catal B* 2014;146:289–297.

22. Li G, Li N, Yang J, Li L, Wang A, Wang X, Cong Y, Zhang T. Synthesis of renewable diesel range alkanes by hydrodeoxygenation of furans over Ni/Hβ under mild conditions. *Green Chem.* 2014;16: 594–599.
23. Li M, Li G, Li N, Wang A, Dong W, Wang X, Cong Y. Aqueous phase hydrogenation of levulinic acid to 1,4-pentanediol. *Chem Commun.* 2014;50: 1414–1416.
24. Saka S, Ueno T. Chemical conversion of various celluloses to glucose and its derivatives in supercritical water. *Cellulose* 1999;6:177–191.
25. Cantero DA, Bermejo MD, Cocero MJ. Kinetic analysis of cellulose depolymerization reactions in near critical water. *J Supercrit Fluids* 2013;75:48–57.
26. Sasaki M, Zhen F, Fukushima Y, Adschiri T, Arai K. Dissolution and hydrolysis of cellulose in subcritical and supercritical water. *Ind Eng Chem Res.* 2000;39:2883–2890.
27. Sasaki M, Adschiri T, Arai K. Kinetics of cellulose conversion at 25 MPa in sub- and supercritical water. *AIChE J*. 2004;50:191–202.
28. Gurgel L, Marabezi K, Zanbom M, Curvelo A. Dilute acid hydrolysis of sugar cane bagasse at high temperatures: a kinetic study of cellulose saccharification and glucose decomposition. *Part I: sulfuric acid as the catalyst*. *Ind Eng Chem Res.* 2012;51:1173–1185.
29. Yu Y, Wu H. Effect of ball milling on the hydrolysis of microcrystalline cellulose in hot-compressed water. *AIChE J*. 2011;57:793–800.
30. Fukuoka A, Dhepe PL. Catalytic conversion of cellulose into sugar alcohols. *Angew Chem Int Ed.* 2006;45:5161–5163.
31. Luo C, Wang S, Liu H. Cellulose conversion into polyols catalyzed by reversibly formed acids and supported ruthenium clusters in hot water. *Angew Chem Int Ed.* 2007;119:7780–7783.
32. Ji N, Zhang T, Zheng M, Wang A, Wang H, Wang X, Chen J. Direct catalytic conversion of cellulose into ethylene glycol using nickel-promoted tungsten carbide catalysts. *Angew Chem Int Ed.* 2008;47:8510–8513.
33. Deng W, Tan X, Fang W, Zhang Q, Wang Y. Conversion of cellulose into sorbitol over carbon nanotube-supported ruthenium catalyst. *Catal Lett*. 2009;133:167–174.
34. Ding L, Wang A, Zheng M, Zhang T. Selective transformation of cellulose into sorbitol by using a bifunctional nickel phosphide catalyst. *ChemSusChem.* 2010;3:818–821.
35. Zhang Y, Wang A, Zhang T. A new 3D mesoporous carbon replicated from commercial silica as a catalyst support for direct conversion of cellulose into ethylene glycol. *Chem Commun.* 2010;46:862–864.
36. Deng W, Liu M, Tan X, Zhang Q, Wang Y. Conversion of cellobiose into sorbitol in neutral water medium over carbon nanotube-supported ruthenium catalysts. *J Catal.* 2010;271:22–32.
37. Geboers J, Van de Vyver S, Carpentier K, de Blochouse K, Jacobs P, Sels B. Efficient catalytic conversion of concentrated cellulose feeds to hexitols with heteropoly acids and Ru on carbon. *Chem Commun.* 2010;46:3577–3579.
38. Zheng M, Wang A, Ji N, Pang J, Wang X, Zhang T. Transition metal–tungsten bimetallic catalysts for the conversion of cellulose into ethylene glycol. *ChemSusChem.* 2010;3:63–66.
39. Pang J, Zheng M, Wang A, Zhang T. Catalytic hydrogenation of corn stalk to ethylene glycol and 1,2-propylene glycol. *Ind Eng Chem Res.* 2011;50:6601–6608.
40. Li C, Zheng M, Wang A, Zhang T. One-pot catalytic hydrocracking of raw woody biomass into chemicals over supported carbide catalysts: simultaneous conversion of cellulose, hemicellulose and lignin. *Energy Environ Sci*. 2012;5:6383–6390.
41. Zhou L, Wang A, Li C, Zheng M, Zhang T. Selective production of 1, 2-propylene glycol from Jerusalem artichoke tuber on Ni-W_2C/AC catalysts. *ChemSusChem.* 2012;5:932–938.
42. Liu Y, Luo C, Liu H. Tungsten trioxide promoted selective conversion of cellulose into propylene glycol and ethylene glycol on a ruthenium catalyst. *Angew Chem Int Ed.* 2012;51:3249–3253.
43. Wang X, Meng L, Wu F, Jiang Y, Wang L, Mu X. Efficient conversion of microcrystalline cellulose to 1,2-alkanediols over supported Ni catalysts. *Green Chem.* 2012;14:758–765.
44. Ji N, Zheng M, Wang A, Zhang T, Chen J. Nickel-promoted tungsten carbide catalysts for cellulose conversion: effect of preparation methods. *ChemSusChem.* 2012;5:939–944.
45. Pang J, Wang A, Zheng M, Zhang Y, Huang Y, Chen X, Zhang T. Catalytic conversion of cellulose to hexitols with mesoporous carbon supported Ni-based bimetallic catalysts. *Green Chem.* 2012;14:614–617.
46. Tai Z, Zhang J, Wang A, Zheng M, Zhang T. Temperature-controlled phase-transfer catalysis for ethylene glycol production from cellulose. *Chem Commun.* 2012;48:7052–7054.
47. Xi J, Zhang Y, Xia Q, Liu X, Ren, J, Lu G, Wang Y. Direct conversion of cellulose into sorbitol with high yield by a novel mesoporous niobium phosphate supported Ruthenium bifunctional catalyst. *Appl Catal A* 2013;459:52–58.
48. Chen J, Wang S, Huang J, Chen L, Ma L, Huang X. Conversion of cellulose and cellobiose into sorbitol catalyzed by ruthenium supported on a polyoxometalate/metal-organic framework hybrid. *ChemSusChem.* 2013;6:1545–1555.
49. Tai Z, Zhang J, Wang A, Pang J, Zheng M, Zhang T. Catalytic conversion of cellulose to ethylene glycol over a low-cost binary catalyst of Raney Ni and tungstic acid. *ChemSusChem.* 2013;6:652–658.
50. Xiao Z, Jin S, Pang M, Liang C. Conversion of highly concentrated cellulose to1,2-propanediol and ethylene glycol over highly efficient CuCr catalysts. *Green Chem.* 2013;15:891–895.
51. Wang A, Zhang T. One-pot conversion of cellulose to ethylene glycol with multifunctional tungsten-based catalysts. *Acc Chem Res.* 2013;46:1377–1386.
52. Zhao G, Zheng M, Zhang J, Wang A, Zhang T. Catalytic conversion of concentrated glucose to ethylene glycol with semi-continuous reaction system. *Ind Eng Chem Res.* 2013;52:9566−9572.
53. Déchamp N, Gamez A, Perrard A, Gallezot P. Kinetics of glucose hydrogenation in a trickle-bed reactor. *Catal Today* 1995;24:29–34.
54. Ju F, VanderVelde D, Nikolla E. Molybdenum-based polyoxometalates as highly active and selective catalysts for the epimerization of aldoses. *ACS Catal*. 2014;4:1358−1364.
55. Kemmer G, Keller S. Nonlinear least-squares data fitting in Excel spreadsheets. *Nat Protoc*. 2010;5:267–280.
56. Kim Y, Kreke T, Ladisch MR. Reaction mechanisms and kinetics of xylo-oligosaccharide hydrolysis by dicarboxylic acids. *AIChE J*. 2013;59:188–199.
57. Chapelle S, Verchère J. Tungstate complexes of aldoses and ketoses of the lyxo series. Multinuclear NMR evidence for chelation by one or two oxygen atoms borne by the side chain of the furanose ring. *Carbohydr Res.* 1995;277:39–50.
58. Chapelle S, Verchère J. Tungsten-183 NMR studies of tungstate complexes of carbohydrates. 1. Characterization of two structural types in the alditol series. Evidence that the tungstate and molybdate threo complexes are not homologous. *Inorg Chem.* 1992;31:648–652.
59. Kishida H, Jin F, Yan X, Moriya T, Enomoto H. Formation of lactic acid from glycolaldehyde alkaline hydrothermal reaction. *Carbohydr Res*. 2006;341:2619–2623.
60. Delidovich IV, Simonov AN, Pestunova OP, and Parmon VN. Catalytic condensation of glycolaldehyde and glyceraldehyde with formaldehyde in neutral and weakly alkaline aqueous media: Kinetics and Mechanism. *Kinet Catal*. 2009;50:297–303.
61. Yan XY, Jin FM, Tohji K, Kishita A, Enomoto H. Hydrothermal conversion of carbohydrate biomass to lactic acid. *AIChE J*. 2010; 56:2727–2733.

Manuscript received Feb. 24, 2014, and revision received June 1, 2014.